nature materials

LETTERS

PUBLISHED ONLINE: 28 FEBRUARY 2010 | DOI: 10.1038/NMAT2703

Ferroelastic switching for nanoscale non-volatile magnetoelectric devices

S. H. Baek[1], H. W. Jang[1], C. M. Folkman[1], Y. L. Li[2], B. Winchester[2], J. X. Zhang[3], Q. He[3], Y. H. Chu[3], C. T. Nelson[4], M. S. Rzchowski[5], X. Q. Pan[4], R. Ramesh[3], L. Q. Chen[2] and C. B. Eom[1]*

Multiferroics, where (anti-) ferromagnetic, ferroelectric and ferroelastic order parameters coexist[1–5], enable manipulation of magnetic ordering by an electric field through switching of the electric polarization[6–9]. It has been shown that realization of magnetoelectric coupling in a single-phase multiferroic such as $BiFeO_3$ requires ferroelastic (71°, 109°) rather than ferroelectric (180°) domain switching[6]. However, the control of such ferroelastic switching in a single-phase system has been a significant challenge as elastic interactions tend to destabilize small switched volumes, resulting in subsequent ferroelastic back-switching at zero electric field, and thus the disappearance of non-volatile information storage[10,11]. Guided by our phase-field simulations, here we report an approach to stabilize ferroelastic switching by eliminating the stress-induced instability responsible for back-switching using isolated monodomain $BiFeO_3$ islands. This work demonstrates a critical step to control and use non-volatile magnetoelectric coupling at the nanoscale. Beyond magnetoelectric coupling, it provides a framework for exploring a route to control multiple order parameters coupled to ferroelastic order in other low-symmetry materials.

There are two important requirements to achieve switchable, non-volatile magnetoelectric devices with multiferroics. First, it is necessary to selectively control the switching path. Second, the switched domain must be stabilized. The first point arises in multiferroics because each switching path can generate different changes in the magnetic order, and some switching paths may not affect the magnetic order at all. This is particularly relevant when magnetic and electric orders are coupled through partial ferroelasticity[10]. In this case, only ferroelastic switching can be used.

The second requirement arises because local ferroelastic switching may produce a high-energy domain state, leading to a relaxation of the smaller (switched) domain back to the original ferroelastic state[10,11]. This would disable long-term storage of information because the magnetic order also relaxes. This phenomenon can potentially occur for all ferroelastic multiferroics such as boracites ($M_3B_7O_{13}X$ with M: Cr, Mn, Fe, Co, Cu, Ni and X: Cl, Br, I), $BaMF_4$ compounds with M: Mg, Mn, Fe, Co, Ni, Zn, molybates ($Tb_2(MoO_4)_3$ and $Gd_2(MoO_4)_3$), phosphates ($LiCoPO_4$) and magnetite (Fe_3O_4; refs 1, 10, 12).

We study these issues in $BiFeO_3$, one of the most promising candidates for magnetoelectric devices as a room-temperature multiferroic system[9]. Figure 1 shows the detailed coupling structure of ferroelectric, antiferromagnetic and ferroelastic orders. If the electric polarization is switched with an external electric field, the rhombohedral $BiFeO_3$ can locally either preserve the ferroelastic state with an electric polarization antiparallel to the original one (Fig. 1b, ferroelectric switching or 180° polarization reversal) or transition to a different ferroelastic state with a different distortion axis (Fig. 1c, ferroelastic switching or 71° polarization reversal). As only the latter type of switching can change the plane of the antiferromagnetic order, 180° polarization switching should be avoided. A recent *ab initio* study of polarization switching paths in $BiFeO_3$ predicts reorientation of the antiferromagnetic plane by 71° polarization switching under [001] electric fields[13]. Similarly, 109° switching also allows magnetoelectric switching because it is another type of ferroelastic domain switching (not shown here). This electrically switched antiferromagnetism can be implemented in magnetoelectric devices using exchange bias with another ferromagnetic layer[14–18]. However, as discussed above, local switching of the electric polarization in this way locally switches the ferroelastic state, nucleating high-energy walls with the surrounding domain. This leaves the switched domain subject to relaxation.

A possible way was reported to stabilize such a ferroelastic switching from relaxation by writing further domains locally by piezoresponse force microscopy (PFM) that surround switched regions in (110) $BiFeO_3$ thin films[11], which is not practical for large-scale device applications. Here we reveal the polarization switching path in monodomain (001) $BiFeO_3$ thin films under a [001] electric field, showing that the dynamics of the switching path changes dramatically with domain size. Moreover, we demonstrate robust ferroelastic switching by fabricating $BiFeO_3$ islands, eliminating the high-energy structural domain wall and removing the driving force for relaxation. Our simple and scalable method is directly applicable to a real device.

A key aspect of the present study is our ability to grow essentially single-variant (001) $BiFeO_3$ heterostructures by off-axis sputtering (see Supplementary Information). This results in an atomically smooth surface as shown in Fig. 2a, which reduces any rough surface ambiguities during the PFM measurement. Previous studies were complicated by the complex domain structure of $BiFeO_3$ arising from its low symmetry. For example, a multi-variant $BiFeO_3$ film on a (001) $SrTiO_3$ substrate has a maximum of four structural (ferroelastic) variants and eight ferroelectric variants[19], making it difficult to uniquely characterize the switching behaviour. In addition, a particular domain boundary affects switching dynamics as a leakage path[19,20]. Reciprocal space mapping by four-circle high-resolution X-ray diffraction (XRD; Fig. 2b) and transmission electron microscopy (Fig. 2c) show that our growth method produces a pure monodomain sample.

[1]Department of Materials Science and Engineering, University of Wisconsin-Madison, Madison, Wisconsin 53706, USA, [2]Department of Materials Science and Engineering, Penn State University, University Park, Pennsylvania 16802, USA, [3]Department of Materials Science and Engineering, University of California, Berkeley, California 94720, USA, [4]Department of Materials Science and Engineering, University of Michigan, Ann Arbor, Michigan 48109, USA, [5]Department of Physics, University of Wisconsin-Madison, Madison, Wisconsin 53706, USA. *e-mail: eom@engr.wisc.edu.

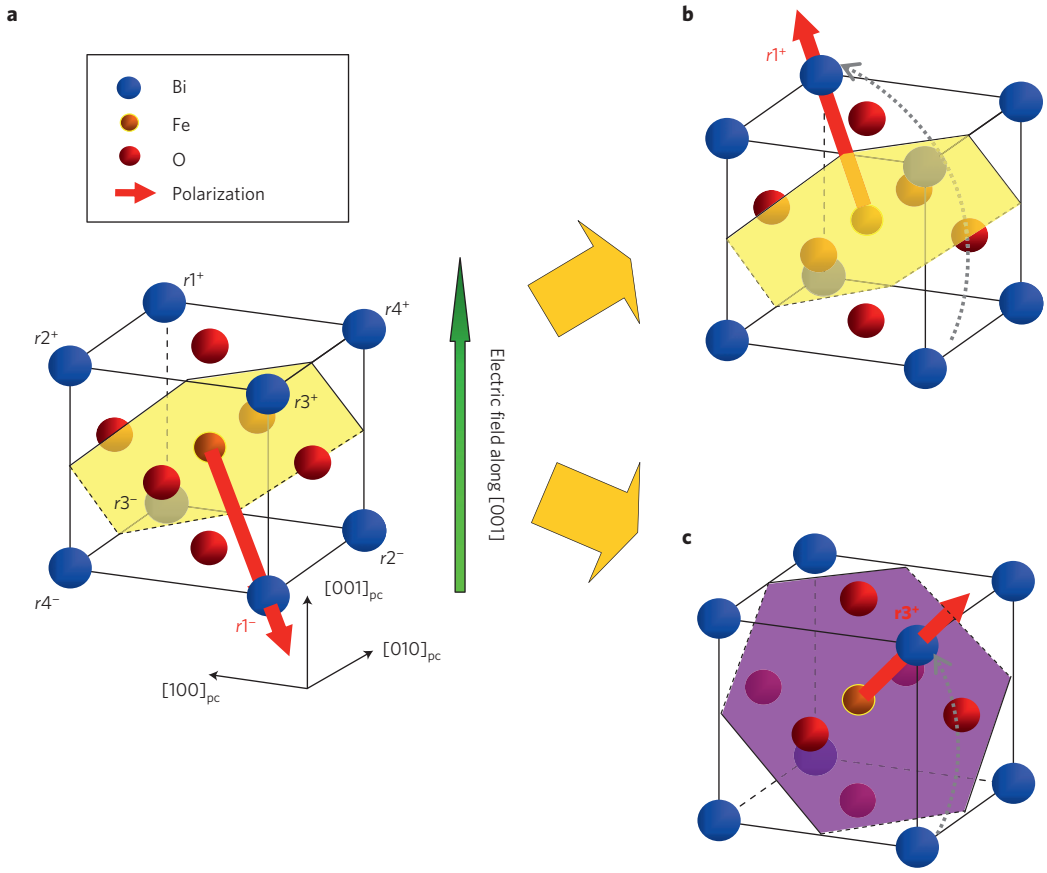

Figure 1 | Magnetoelectric coupling in $BiFeO_3$. a, The coupling between polarization and antiferromagnetic order in $BiFeO_3$ film. The spin cycloid has been believed to be broken in thin films[30]. pc: pseudocubic. **b**,**c**, The magnetoelectric coupling geometry after 180° polarization switching (**b**) and 71° polarization switching (**c**).

Standard polarization–electric-field hysteresis loop measurements demonstrate that the polarization direction is down throughout the sample. The notations for ferroelectric and ferroelastic domains of $BiFeO_3$ thin films are adopted from ref. 21: $r1$, $r2$, $r3$ and $r4$ for ferroelastic domains, and positive (+) and negative (−) signs for ferroelectric 'up' and 'down' states, respectively, as shown in Fig. 1a.

We first use a phase-field simulation approach[22] to predict the preferred switching path of (001) monodomain $BiFeO_3$ films under a [001] electric field. In the $BiFeO_3$ system, the ferroelastic energy contributes significantly to the total energy because of its rhombohedral distortion[23] and substrate strain. The $r1^+$ domain resulting from 180° switching is the most stable because of the absence of structural mismatch with the surrounding unswitched $r1^-$ region, whereas the $r3^+$ domain from 71° switching is the most unstable because of the large structural mismatch. However, we find that the required activation energy for direct 180° switching is much higher than for 71° switching. 180° switching needs to switch all three components of polarization, whereas 71° switching needs to switch only the vertical component. Moreover, an applied field along the [001] direction on (001) $BiFeO_3$ films is effectively applied to switch the vertical component, and does not have a direct driving force to switch in-plane components of polarization because of the relative geometry between the applied field and polarization. On the basis of this phase-field result, the polarization-switching diagram can be described as shown in Fig. 3. It suggests that direct 180° switching is kinetically suppressed because of its high activation barrier. Instead, a new polarization-switching path is predicted: relaxation-mediated 180° switching. The applied electric field induces 71° switching, and the unstable $r3^+$ domain subsequently relaxes into the stable $r1^+$ state in the absence of an electric field, resulting in 180° switching finally.

There are two possible ferroelastic relaxation paths of a 71°-switched domain ($r3^+$): from $r3^+$ to $r1^-$ or from $r3^+$ to $r1^+$. Our phase-field simulation results show $r3^+$ to $r1^+$ relaxation on a (001) $SrTiO_3$ substrate, resulting in 180° domains, rather than direct relaxation to the matrix domain through the $r3^+$ to $r1^-$ path. Thermodynamic consideration alone does not explain this 'unexpected' switching. We attribute this phenomenon to kinetic reasons; that is, it is easier to relax kinetically to the 180° domain rather than the as-grown matrix domain. The biaxial compressive strain imposed by the substrate on the $BiFeO_3$ film distorts the rhombohedral unit cell, resulting in shorter in-plane lattice parameters and an elongated out-of-plane lattice parameter. This strain results in the preferential 180° relaxation. We also carried out phase-field simulations for ferroelastic relaxation under biaxial tensile strain. Tensile strain distorts the rhombohedral unit cell, resulting in elongated in-plane lattice parameters and a shorter out-of-plane lattice parameter. The simulation shows that a 71°-switched domain under tensile strain follows the $r3^+$ to $r1^-$ relaxation path, switching back to the matrix domain.

Our phase-field simulations also reveal that ferroelastic relaxation proceeds preferentially from the domain boundary by replacing the unstable domain with the stable one. The stable domain ($r1^+$) is formed at the boundary, and propagates into the unstable domain ($r3^+$). The simulations indicated that this non-uniform transformation process is domain-size dependent because the portion of the domain wall, which is the active region of domain relaxation, is inversely proportional to domain size. Thus,

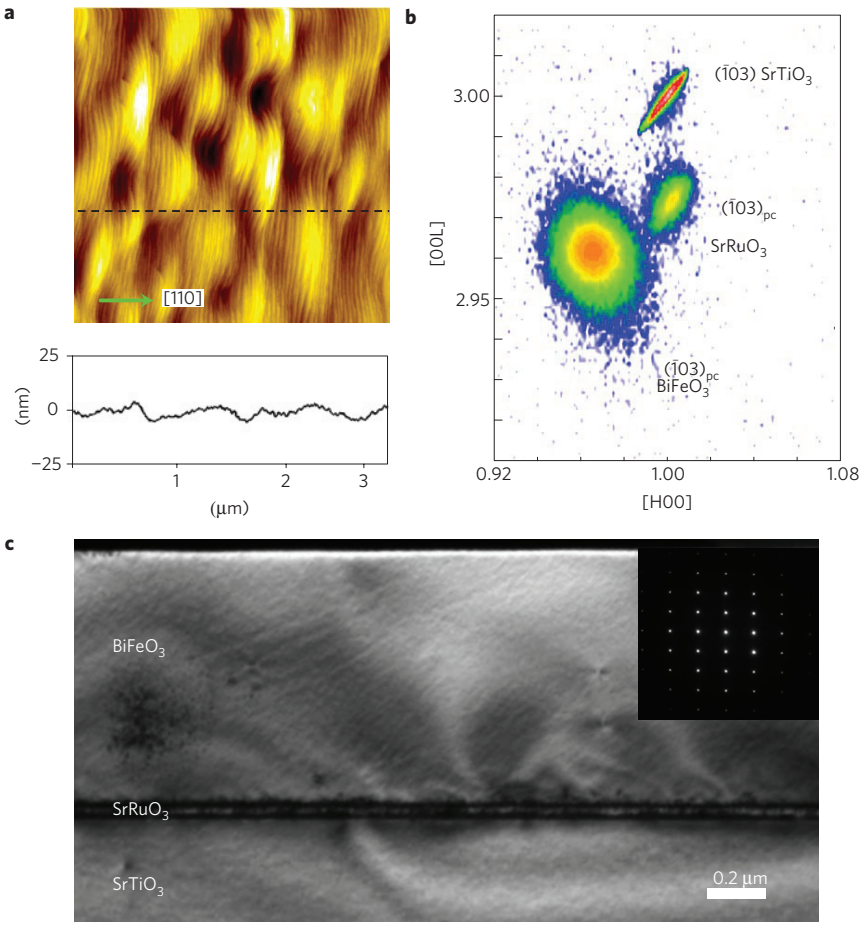

Figure 2 | Monodomain (001) $BiFeO_3$ thin films. a, Surface morphology of a monodomain $BiFeO_3$ thin film measured by atomic force microscopy. The steps have 2 or 3 unit-cell height because of the step bunching resulting from the high angle (4°) of substrate miscut. **b**, Reciprocal space mapping of $\bar{1}03$ peaks. **c**, Cross-sectional transmission electron microscopy image with a $[\bar{1}10]$ zone axis. The inset is the selected-area electron diffraction image of the $BiFeO_3$ region.

the smaller the $r3^+$ domains are in the matrix of $r1^-$, the shorter the relaxation time is expected to be.

To examine these theoretical predictions in real time, we used XRD for large size domains. The relatively large rhombohedral distortion ($\alpha = 89.4°$) of $BiFeO_3$ permits us to easily distinguish different ferroelastic domains. Areas of 200 μm × 700 μm size are switched by applying a negative electric field with Pt top electrodes. After polarization switching, XRD mapping around the $\bar{1}\bar{1}3$ substrate peak shows that a new ferroelastic domain ($r3^+$) of $BiFeO_3$ has evolved, which indicates polarization is switched by 71°, with no observation of 180° switching. This 71° switching path is reversible by applying a positive electric field, and repeatable over many cycles. The intensity of the $BiFeO_3$ 113_{pc} peak from the $r3^+$ domain, directly proportional to the domain volume, was monitored as a function of time as shown in Fig. 4a. Clearly, 71° switching is observed, as predicted by the phase-field simulations, and large-area ferroelastic switching is stable throughout the 24 h of the experiment.

However, this stability does not extend to small domain sizes. We used PFM to switch areas with dimensions of a few micrometres by applying an electric field by means of the conductive PFM tip. Subsequently, the domain structure was monitored as a function of time. Figure 4b shows ferroelastic relaxation with time for $r3^+$ domains of different sizes. The in-plane PFM image in the inset of Fig. 4b shows the contrast change of a 3 × 3 μm size $r3^+$ domain from dark to bright after 2 h, which corresponds to a transition from the initial $r3^+$

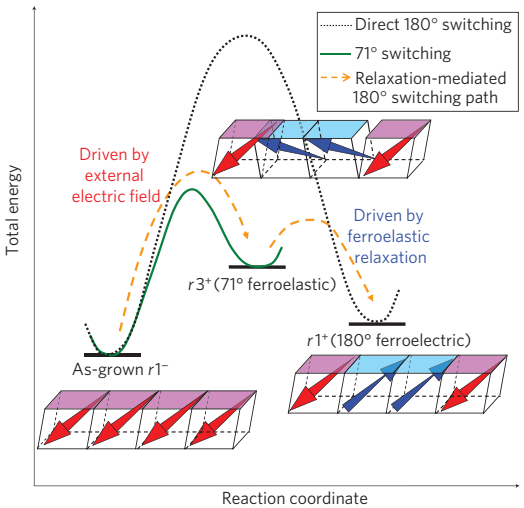

Figure 3 | Schematic illustration of the ferroelectric switching path of $BiFeO_3$ thin films predicted by phase-field calculations. Direct 180° polarization switching is not kinetically favourable because of the high activation barrier. Instead, the ferroelastic relaxation-mediated 180° switching path through 71° switching is expected. The diagrams show the high-energy state of the domain walls resulting from disorientation of unit cells in ferroelastic switching, and the low-energy state after relaxation into 180° switching.

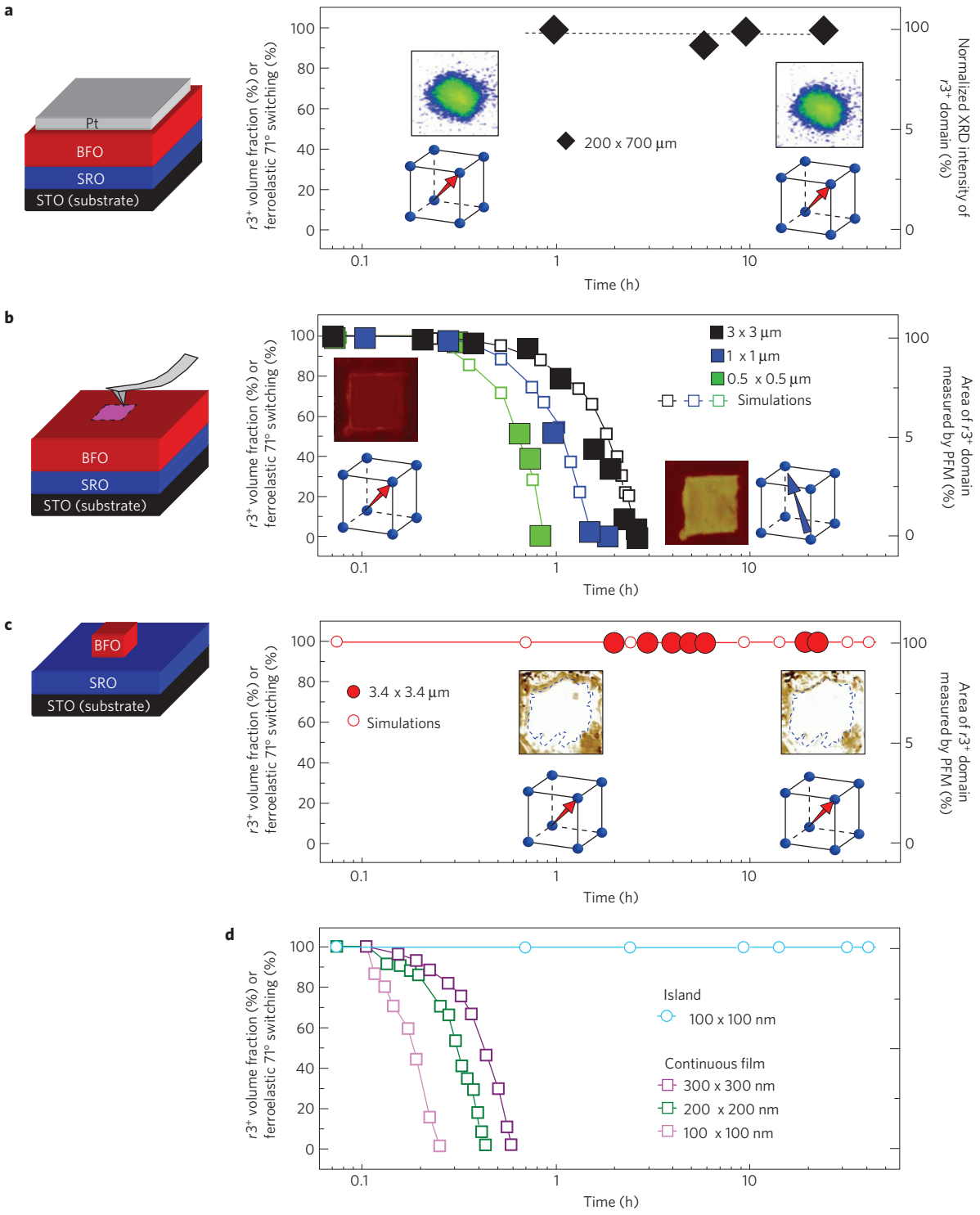

Figure 4 | Enhanced stability of ferroelastic switching by a $BiFeO_3$ island. a, 113_{pc} peak intensity of the $r3^+$ domain as a function of time after polarization switching of a 200 × 700 μm area by the top electrode. The inset is an XRD peak of 113_{pc} $BiFeO_3$. **b**, $r3^+$ domain area change by PFM imaging as a function of time after switching of 3 × 3 μm, 1 × 1 μm and 0.5 × 0.5 μm areas by the PFM tip. **c**, $r3^+$ domain area change of an island with 3.4 × 3.4 μm area as a function of time. The insets of **b** and **c** are the in-plane PFM images. **d**, Phase-field simulation results on the nanometre scale for ferroelastic relaxation in films and an island. The diagrams on the left describe the samples measured (continuous film in **a**,**b** and patterned island in **c**). BFO: $BiFeO_3$, SRO: $SrRuO_3$ and STO: $SrTiO_3$.

domain (71° switching) to the $r1^+$ domain (180° switching). Furthermore, the relaxation rate increases markedly with decreasing initial domain size. These results are consistent with our theoretical prediction as shown in Fig. 3. As the micrometre size range is too large for phase-field simulation, the data in Fig. 4 are plotted by fitting simulation data with the same area ratio to experimental data. Some part of the $r3^+$ domains near the domain boundary is relaxed to $r1^-$ through $r1^+$, resulting in shrinkage of the total volume, which is due to the small scale of simulation. Other supportive evidence for this switching path

is the field-dependence behaviour by PFM tip switching: 180° switching by low electric field and 71° switching by high field, which is consistent with previously reported PFM works on $BiFeO_3$ films[10,24]. The role of high field is to increase the switching area under the PFM tip[25,26], which slows down the relaxation process during domain writing (see Supplementary Information). Our results are distinctively different from a previous report[27] on intermediate non-180° switching during 180° polarization reversal in rhombohedral $(111)_{pc}$ $Pb(Zn_{1/3}Nb_{2/3})O_3$–$PbTiO_3$ single crystals with multiple domains under an electric field in the $[111]_{pc}$ direction. Our ferroelastic relaxation occurs under zero electric field.

These results indicate that for both non-volatile storage as well as magnetoelectric coupling, the switched domain must be large to slow down the relaxation process, which is not desirable for high-density memory applications. However, the nature of the domain switching path, as shown in Fig. 3, provides a possible way to achieve both selective control and stabilization of ferroelastic 71° switching by suppressing the relaxation process. As revealed by the simulations, the origin of relaxation is the high-energy domain walls with structural distortions between the switched and the unswitched regions. Those boundaries can be removed simply by eliminating the matrix (unswitched) region. Here we have demonstrated stable 71° switching by fabricating $BiFeO_3$ islands, the side walls of which are free surfaces without any mechanical stress. The heterostructure of (001) monodomain $BiFeO_3$ thin film with a platinum top layer is ion-milled down to a $BiFeO_3/SrRuO_3$ interface with a lithographically patterned photoresist mask. The polarization of the island is switched by applying an electric field between the top and bottom electrodes. The top Pt electrode is then removed, and the domain structure is imaged by PFM as a function of time. Figure 4c shows a pronounced enhancement of ferroelastic ($r3^+$) switching stability in a $3.4 \times 3.4\,\mu m$ island compared with a similar sized domain in a continuous thin film (Fig. 4b). The island sustains ferroelastic 71° switching even after 26 h without relaxation, whereas a domain with similar size in a continuous film is fully relaxed after only two hours. This experimental result on $BiFeO_3$ islands is also consistent with our theoretical prediction. To check the validity of this method at the nanometre scale, where direct experiments are challenging, phase-field simulations were carried out. Figure 4d shows possible relaxation behaviours of nanometre-sized domains in both continuous $BiFeO_3$ films and a 100×100 nm large $BiFeO_3$ island. It is interesting to note that the $BiFeO_3$ island has stable ferroelastic switching, whereas continuous films have a faster relaxation.

There are several unique advantages of this island structure. First, it fundamentally can be scaled down, constrained only by nanofabrication technology[28], which might lead to high-density memory devices. Second, by controlling the shape, sidewall orientation and crystallographic orientation of the island, this method can be applied to other multiferroics where the magnetic and electric orders are coupled in their own unique ways. Third, our island structure can reduce noise signals coming from undesirable domain switching. In ferroelastic materials, mechanical cross-talk, the formation of undesirable domains to release elastic and electric energy, can occur near ferroelastic domain boundaries[9]. These undesirable domains contain a different magnetoelectric coupling geometry than desired, distorting stored information. Fourth, it can reduce the operating voltage. The vertical capacitor structure requires an electric field only just above the coercive field whereas localized probe switching needs a higher field to stabilize ferroelastic switching. Moreover, we can expect that the high aspect ratio may reduce the coercive field as demonstrated in ref. 29.

We have demonstrated that the stability of the switched state in multiferroic $BiFeO_3$ thin films is sensitive to the lateral constraints that are imposed on it. Eliminating the constraints imposed by the surrounding matrix has a significant effect on the stability of the switched state. This work opens a new avenue to designing magnetoelectric coupling routes and device geometries to realize non-volatile magnetoelectric coupling devices at the nanoscale. Beyond magnetoelectric coupling, it provides a framework for exploring routes to control multiple order parameters coupled to ferroelastic order in other low-symmetry materials.

Received 7 October 2009; accepted 25 January 2010; published online 28 February 2010

References

1. Fiebig, M. Revival of the magnetoelectric effect. *J. Phys. D* **38,** R123–R152 (2005).
2. Spaldin, N. A. & Fiebig, M. The renaissance of magnetoelectric multiferroics. *Science* **309,** 391–392 (2005).
3. Eerenstein, W., Mathur, N. D. & Scott, J. F. Multiferroic and magnetoelectric materials. *Nature* **44,** 759–765 (2006).
4. Kimura, T. *et al.* Magnetic control of ferroelectric polarization. *Nature* **426,** 55–58 (2003).
5. Hur, N. *et al.* Electric polarization reversal and memory in a multiferroic material induced by magnetic fields. *Nature* **429,** 392–395 (2004).
6. Zhao, T. *et al.* Electrical control of antiferromagnetic domains in multiferroic $BiFeO_3$ films at room temperature. *Nature Mater.* **5,** 823–829 (2006).
7. Chu, Y.-H. *et al.* Electric-field control of local ferromagnetism using a magnetoelectric multiferroic. *Nature Mater.* **7,** 478–482 (2008).
8. Lebeugle, D. *et al.* Electric-field-induced spin flop in $BiFeO_3$ single crystals at room temperature. *Phys. Rev. Lett.* **100,** 227602 (2008).
9. Catalan, G. & Scott, J. F. Physics and applications of bismuth ferrite. *Adv. Mater.* **21,** 2463–2485 (2009).
10. Schmid, H. Some symmetry aspects of ferroics and single phase multiferroics. *J. Phys. Condens. Matter* **20,** 434201 (2008).
11. Cruz, M. P. *et al.* Strain control of domain-wall stability in epitaxial $BiFeO_3$(110) films. *Phys. Rev. Lett.* **99,** 217601 (2007).
12. Schmid, H. On the possibility of ferromagnetic, antiferromagnetic, ferroelectric, and ferroelastic domain reorientations in magnetic and electric fields. *Ferroelectrics* **221,** 9–17 (1999).
13. Lisenkov, S., Rahmedov, D. & Bellaiche, L. Electric-field-induced paths in multiferroic $BiFeO_3$ from atomistic simulations. *Phys. Rev. Lett.* **103,** 047204 (2009).
14. Bibes, M. & Barthelemy, A. Multiferroics: Towards a magnetoelectric memory. *Nature Mater.* **7,** 425–426 (2008).
15. Bea, H. *et al.* Tunnel magnetoresistance and robust room temperature exchange bias with multiferroic $BiFeO_3$ epitaxial thin films. *Appl. Phys. Lett.* **89,** 242114 (2006).
16. Dho, J., Qi, X., Kim, H., MacManus-Driscoll, J. L. & Blamire, M. G. Large electric polarization and exchange bias in multiferroic $BiFeO_3$. *Adv. Mater.* **18,** 1445–1448 (2006).
17. Bea, H., Gajek, M., Bibes, M. & Barthelemy, A. Spintronics with multiferroics. *J. Phys. Condens. Matter* **20,** 434231 (2008).
18. Martin, L. W. *et al.* Nanoscale control of exchange bias with $BiFeO_3$ thin films. *Nano Lett.* **8,** 2050–2055 (2008).
19. Jang, H. W. *et al.* Domain engineering for enhanced ferroelectric properties of epitaxial (001) $BiFeO_3$ thin films. *Adv. Mater.* **21,** 817–823 (2009).
20. Seidel, J. *et al.* Conduction at domain walls in oxide multiferroics. *Nature Mater.* **8,** 229–234 (2009).
21. Streiffer, S. K. *et al.* Domain patterns in epitaxial rhombohedral ferroelectric films. I. Geometry and experiments. *J. Appl. Phys.* **83,** 2742–2753 (1998).
22. Li, Y. L., Hu, S. Y., Liu, Z. K. & Chen, L. Q. Effect of substrate constraint on the stability and evolution of ferroelectric domain structures in thin films. *Acta Mater.* **50,** 395–411 (2002).
23. Khachaturyan, A. G. *Theory of Structural Transformations in Solids* (John Wiley, 1983).
24. Zavaliche, F. *et al.* Polarization switching in epitaxial $BiFeO_3$ films. *Appl. Phys. Lett.* **87,** 252902 (2005).
25. Paruch, P., Tybell, T. & Triscone, J. M. Nanoscale control of ferroelectric polarization and domain size in epitaxial $Pb(Zr_{0.2}Ti_{0.8})O_3$ thin films. *Appl. Phys. Lett.* **79,** 530–532 (2001).
26. Kalinin, S. V. *et al.* Intrinsic single-domain switching in ferroelectric materials on a nearly ideal surface. *Proc. Natl Acad. Sci. USA* **104,** 20204–20209 (2007).
27. Daniels, J. E. *et al.* Neutron diffraction study of the polarization reversal mechanism in $[111]_c$-oriented $Pb(Zn_{1/3}Nb_{2/3})O_{3-x}PbTiO_3$. *J. Appl. Phys.* **101,** 104108 (2007).
28. Ruzmetov, D. *et al.* Epitaxial magnetic perovskite nanostructures. *Adv. Mater.* **17,** 2869–2872 (2005).

29. You, C. C. *et al*. The fabrication and characterization of $PbTiO_3$ nanomesas realized on nanostructured $SrRuO_3/SrTiO_3$ templates. *Nanotechnology* **20,** 255705 (2009).
30. Bai, F. *et al*. Destruction of spin cycloid in $(111)_c$-oriented $BiFeO_3$ thin films by epitaxial constraint: Enhanced polarization and release of latent magnetization. *Appl. Phys. Lett.* **86,** 032511 (2005).

Acknowledgements

The authors gratefully acknowledge the financial support of the National Science Foundation through grant ECCS-0708759, the Office of Naval Research through grant N00014-07-1-0215 and a David and Lucile Packard Fellowship (C.B.E.). The theoretical analyses and phase-field simulations at Penn State were supported by DOE Basic Sciences under grant number DE-FG02-07ER46417 (L.Q.C.) and NSF MRSEC on Nanosciences under grant number NSF DMR-0820404 (Y.L.L. and B.W.). The work at the University of Michigan was supported by DOE Basic Sciences under grant number DE-FG02-07ER46416 (X.Q.P.). The work at Berkeley is supported by the Director, Office of Science, Office of Basic Energy Sciences, Materials Sciences Division of the US Department of Energy under contract No. DE-AC02-05CH1123. The authors thank T. Tybell for helpful discussions.

Author contributions

S.H.B. fabricated samples and prepared the manuscript. H.W.J. and C.M.F. analysed the symmetry of $BiFeO_3$ by XRD. Y.L.L. and B.W. carried out phase-field simulations. J.X.Z., Q.H. and Y.H.C. carried out high-field PFM measurements. C.T.N. and X.Q.P. carried out TEM measurements. C.B.E., R.R., L.Q.C., M.S.R. and X.Q.P. supervised the experiments and contributed to manuscript preparation. C.B.E. designed and directed the research. All authors discussed the results and implications and commented on the manuscript at all stages.

Additional information

The authors declare no competing financial interests. Supplementary information accompanies this paper on www.nature.com/naturematerials. Reprints and permissions information is available online at http://npg.nature.com/reprintsandpermissions. Correspondence and requests for materials should be addressed to C.B.E.